J MATER SCI **41** (2006) 763–777

The effect of electric field and pressure on the synthesis and consolidation of materials: A review of the spark plasma sintering method

Z. A. MUNIR[*], U. ANSELMI-TAMBURINI[†]
Department of Chemical Engineering and Materials Science, University of California, Davis, CA, 95616, USA

M. OHYANAGI
Department of Materials Chemistry, Ryukoku University, Ohtsu, Japan

The use of electric current to activate the consolidation and reaction-sintering of materials is reviewed with special emphasis of the spark plasma sintering method. The method has been used extensively over the past decade with results showing clear benefits over conventional methods. The review critically examines the important features of this method and their individual roles in the observed enhancement of the consolidation process and the properties of the resulting materials. © *2006 Springer Science + Business Media, Inc.*

1. Historical background

Sintering as an art had origins that are thousands of years old. The formation of bricks by heating clay bodies in an open pit fire is one of the earliest examples of sintering practiced by ancient civilizations of Mesopotamia. The practice is known to have existed as far back as 6000 BC [1]. The ancient Egyptians sintered metals and ceramics as early as 3000 BC and the Incas of South America used sintering to make gold-platinum jewelry. Significant empirically developed advances followed in the production of ceramics in Egypt and Greece and porcelain in the Near East, China, and Europe. Sintering as a solid-state science came out of the empirical work began during the period 1920–1950 [2]. Contributions to the understanding of the basic phenomena of consolidation by mass transport mechanism were subsequently made by Frenkel, Kuczynski, Lenel, Coble, Kingery, German, and others [3–8].

Understanding the basic phenomena and the important parameters governing sintering has led to investigation on means to activate the process. The objective of these investigations was to enhance mass transport to either make possible the sintering of extremely refractory materials or to lower the temperature of consolidation. Examples of the former include activated sintering by addition of a minor phase [9] and the motivation for the latter is the need to preserve nanostructure by minimization Ostwald ripening [10].

One of the methods of activating the sintering process involves the use of electrical current. Although the recent widespread use of this approach has been generated by the availability of commercially built devices, its origin is much older. Patents issued as early as 1933 describe methods in which an electric discharge or current is utilized to aid in the sintering of powders or the sinter-joining of metals [11–13]. Subsequent work on what was then called "spark sintering" was done by Lenel at RPI in the 1950s [14], by scientists at Lockheed Missile and Space Company in California [15, 16] and Inoue in Japan in the in the 1960s and 1970s [17, 18]. As will be shown subsequently in this review, the use of a current to aid in the sintering of materials has been applied in a large number of investigations. Commercial units which have been developed over the past few decades include "plasma-assisted sintering" (PAS) [19], "pulsed electric current sintering" (PECS) [20], "electroconsolidation" also known as electric pulse assisted consolidation (EPAC) [21], and "spark plasma sintering" (SPS) [22].

The emerging theme from the large majority of investigations of current activated sintering is that it has decided advantages over conventional methods including pres-

---

[*] Author to whom all correspondence should be addressed.

[†] *Permanent address*: Department of Physical Chemistry, University of Pavia, Pavia, Italy.

0022-2461 © *2006 Springer Science + Business Media, Inc.*
DOI: 10.1007/s10853-006-6555-2

sureless sintering, hot-pressing, and others. These advantages include: lower sintering temperature, shorter holding time, and marked comparative improvements in properties of materials consolidated by this method. Lower temperatures and shorter holding times have made it possible to sinter nanometric powders to near theoretical values with little grain growth [10, 23]. While in most cases the evidence demonstrating the superiority of the current activated sintering is clearly presented, the explanations given to rationalize these advantages fall short of scientific adequacy. In most cases the notion of the existence of plasma is repeated routinely, almost as matter of faith without providing evidence or justification.

In this review we intend to provide a critical discussion of the field activated sintering process, emphasizing fundamental investigations made during the past decade. The review is not intended to cover every paper published on the subject, a task that would be formidable even if it were deemed worthwhile. There are no less than a thousand papers published on this subject during the past decade. Moreover, a review that describes findings and observations only would not be helpful to those interested in the fundamental issues related to this method of activated sintering. As pointed out above, the vast majority of the published papers present results showing improved conditions and properties without delving on the role of the current.

2. Field effects in materials processes

In general the work reported on the use of a current to activate sintering tends to focus on the thermal effects of the current. Joule heating provides high heating rates which can provide a benefit by by-passing the grain coarsening low temperature mechanisms (e.g. surface diffusion) [24, 25]. The effect of the pressure is also cited as aiding in particle re-arrangement which contributes to the enhanced sintering. But by and large, little attention is paid to the intrinsic role of the current. That an electric field (contacting and no-contacting) has an influence on materials processes has been clearly demonstrated in a variety of studies over several decades [26, 27].

The field has been shown to have an effect on: low-angle grain boundary motion in ionic crystals [28], sublimation of alkali halide crystals [29–31], phase transformation in alloys [32, 33], plastic deformation in metals and ceramics [34], hardenability of steel [35], microstructural development in alloys [36], metal nuclei growth on ceramic substrates [37], wave dynamics of self-propagating reactions [38, 39], nucleation of nanocrystallites in bulk metallic glasses [40], nucleation and growth of intermetallics and ceramic phases [41–44], and impregnation of ceramics or glasses with nanocrystalline particles to form functionally-graded materials [45]. In these investigations the applied field was in both contacting and non-contacting modes, with the former thus being a current effect in reality.

The specific role of the field (current) is different depending on the process being affected and on the nature of the material being investigated. Since the focus of this review is on sintering, the effect of the field on mass transport will be the focus of the discussion here. The effect of a field on mass transport can be evaluated form the electromigration theory [46]:

$$J_{\mathrm{i}} = -\frac{D_{\mathrm{i}}C_{\mathrm{i}}}{RT}\left[\frac{RT\,\partial \ln C_{\mathrm{i}}}{\partial x} + Fz^{*}E\right] \tag{1}$$

where J_{i} is the flux of the diffusing ith species, D_{i} is the diffusivity of the species, C_{i} is the concentration of the species, F is Faraday's constant, z^{*} is the effective charge on the diffusing species, E is the field, R is the gas constant, and T is temperature.

However, under the typical current activated sintering (e.g., the spark plasma sintering, SPS) the temperature and current are not independent parameters and thus the thermal effect of the current (Joule heating) cannot unambiguously be separated from the intrinsic role of the current. We have recently designed and conducted experiments in which the intrinsic role of the current can be determined [41–43, 47]. In these experiments we utilized a layer geometry, typically consisting of three layers. One layer of one metal is sandwiched between two layers of another metal and annealed with and without a current at a constant temperature. The results show a remarkable influence of the current on mass transport contributing to the formation of intermetallic phases, as can be seen from Fig. 1 [43, 47]. The three depicted samples for the Al-Au system were annealed at the same temperature (500°C) for the same time (4 h) but under different current densities: in the first part the annealing was done without current while in the second and third parts annealing took place under current with two density levels. It can be clearly seen that the growth of the total intermetallic layer at the Al and Au interefaces is markedly affected by the current. This is better shown quantitatively in Fig. 2 [43, 47] where the growth rate at 400°C (reflected by the slope of the lines) changes depending on the presence and density of the current. In addition to the change in the growth rate, the figure also shows a change in the incubation time for the nucleation of the product layer (within the limits of resolution of measurements). In the absence of a current, the product layer is not measurable until after more than 20 h of annealing. This incubation time for phase nucleation is reduced drastically as the intensity of the current is increased, becoming nearly zero when annealing was done under a current density of 10^3 A.cm^{-2}. Similar observations were made on the system Ni-Ti [42]. In this system a kinetic analysis showed that the intrinsic growth rate constant could be as much as a factor of 40 higher

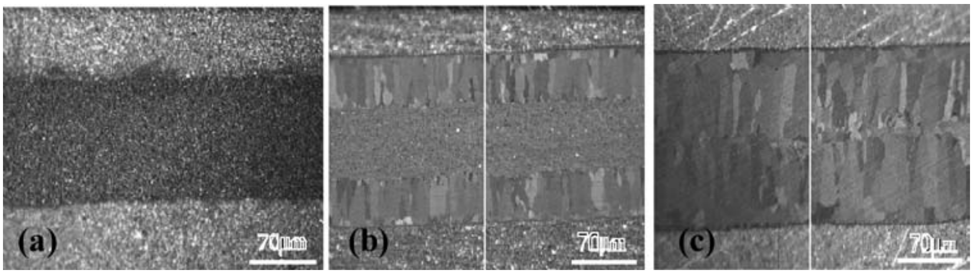

Figure 1 Effect of electric current on growth of intermetallic product layer at two Al/Au interfaces, annealed at 450°C for 4 h (outer layers are Al and inside layer is Au): (a) no current, (b) current density=0.51×10^3 A/cm^2, and (c) current density=1.02×10^3 A/cm^2.

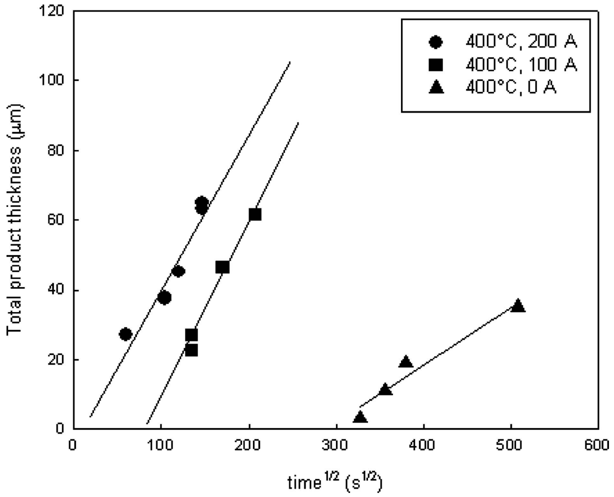

Figure 2 Effect of current on growth rate of intermetallic layer forming between Al and Au layers. Thickness is plotted vs. the square root of time for a parabolic growth.

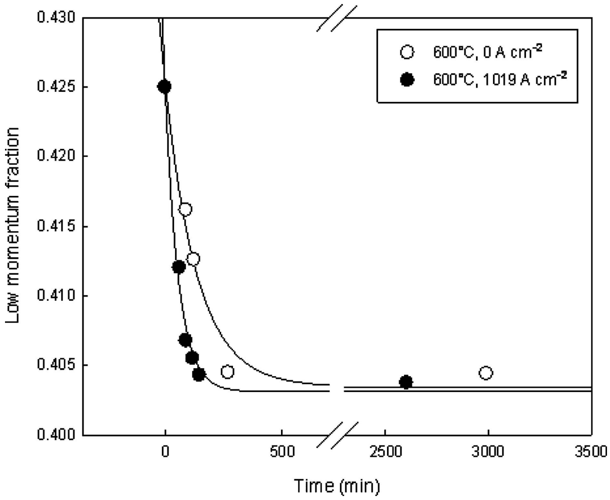

Figure 3 The change in low momentum fraction with time for Ni_3Ti annealed in the presence and absence of a current. The curve indicates the annealing out of point defects in this intermetallic phase with and without a current.

in the case of current annealing relative to current-free annealing. In addition it was demonstrated that the activation energy for the formation of the various phases in this binary decreased with an increase in the intensity of the current.

In the results briefly described above, the direction of the imposed DC current had no effect on the growth of the intermetallics, in contrast to expectations based on electromigration theory [46]. However, as will be seen later, a direct comparison with classical electromigration studies cannot be made since in the situation in this case is complicated by the nucleation of and subsequent diffusion in the new phase. Regardless of this, the results show clearly that the imposition of a current has a pronounced effect on mass transport. Thus the question is: what is the basis of this effect? In other words, what mechanism of mass transport is being affected by the current? In part, the answer for this comes from an earlier study by Kumar *et al.* [48], in which it was shown that the imposition of a current increased the concentration of vacancies in a copper-aluminum alloy. More recent work in our laboratory has provided additional insight on the effect of the current. To avoid the complication of the nucleation of a new phase, the recent work focused on the annealing of quenched-in point defects in an alloy, Ni_3Ti [49]. Using positron annihilation spectroscopy (PAS), it was shown that the imposition of a DC current increased the annealing rate of point defects, as shown in Fig. 3. This was attributed to a 24% decrease in the activation energy of mobility. Lack of a directional dependence on the current was interpreted in terms of an electron wind effect modified by the requirement of maintaining composition in this ordered intermetallic phase.

At the present level of understanding, the observed current's influence on mass transport can be attributed to one of the several intrinsic effects including electron wind modification of the diffusion flux (i.e., electromigration) [47], an increase in point defect concentration [48], or a reduction in the mobility activation energy for defects [49]. The results discussed above were not obtained under SPS conditions. However, as will be discussed in the following section, mass transport enhancement has been observed under the latter condition and the applicability of the interpretation provided for these observations is assumed to be valid under SPS condtions.

3. The spark plasma sintering process: Background

As indicated above, the method used to sinter powders under the effect of current and pressure has been referred to by several names, perhaps the most common of which is spark plasma sintering, or SPS. We note, however, that in more recent publications scientists who used the trademarked SPS equipment refer to their method as pulsed electric current sintering (PECS). This is possibly done to avoid the use of the word plasma whose existence, as pointed out above, has yet to be unambiguously demonstrated. Nevertheless, in this review we will use the SPS designation, since by far the largest number of investigators utilized this rubric in their publications.

The importance of the SPS method as a tool for consolidation of powders process has been demonstrated by the large number of papers published during the past decade. Although excellent short overviews have been published [50, 51], no attempt has been to provide a comprehensive review of the process. Fig. 4a shows a seemingly exponential increase in the number of papers on SPS published since 1994. In that year only a handful of papers were published while in the last year with complete data (2003), more than 150 papers were published. The apparent decrease for the year 2004 reflects an incomplete data at the time this survey was made; the actual final number will likely exceed that of the previous year. Since the effort to commercialize the method was initiated in large scale in Japan, it is not surprising that the vast majority of papers published are from Japan, as can be seen in Fig. 4b. China and Korea are second and third, respectively, while the other countries contributed fewer than about 30 papers each. In part this distribution reflects the availability of the equipment in these countries, with Japan having by far the largest number of SPS units.

The SPS process utilizes pulsed high DC current along with uniaxial pressure to consolidate powders. It is shown schematically in Fig. 5. The success of the process has been highlighted by noteworthy achievements of, for example, cleaner grain boundaries in sintered ceramic materials [52, 53], a remarkable increase in superplasticity of ceramics [54], higher permittivity in ferroelectrics [55], improved magnetic properties [56, 57], improved bonding quality [58], improved thermoelectric properties [59, 60], and reduced impurity segregation at grain boundaries [53]. Furthermore, through the use of prior mechanical activation (high energy milling) on reactant powders, the SPS

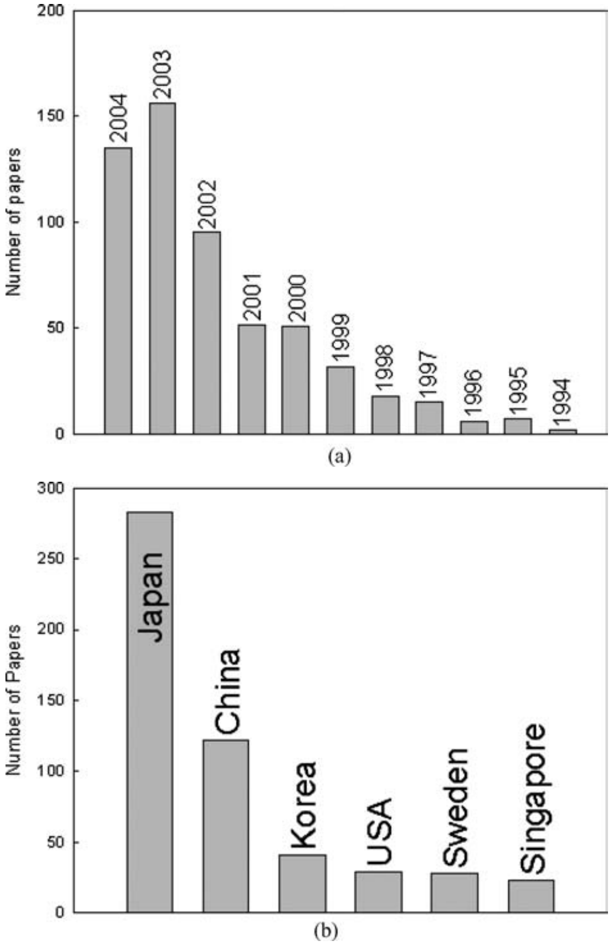

Figure 4 Statistics of publication on the SPS process: (a) Papers published each year since 1994, (b) total publications by country over the same period. Note: the data for 2004 are likely to be incomplete.

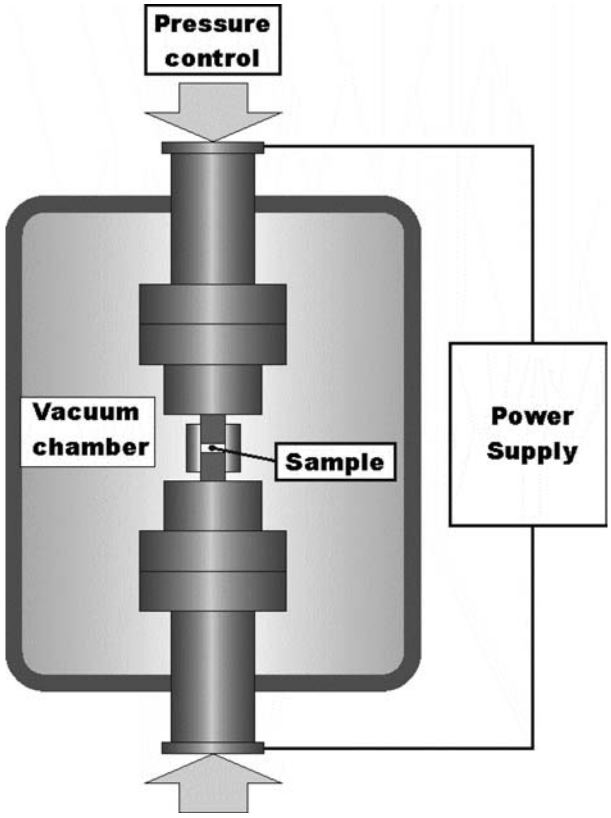

Figure 5 Schematic of the SPS process.

TABLE I Selected examples of the utilization of the SPS method

Material category	Materials investigated	References
Armor materials	Al_2O_3; $(TiB_2)_{0.95}Ti_{0.05}$	69
Biomaterials	Hydroxyapatite	70, 71
Catalysts	Ni-Mo	72
Cellular structures	Ni-P alloy	73
Cemented carbides	WC-Co	74, 75
Composites	TiB_2-TiC; AlN-TiB_2	76, 77
Dielectrics	$Ba_{0.5}Sr_{0.5}TiO_3$; $Ba_{6-3x}Sm_{8+2x}Ti_{18}O_{54}$	78, 79
Electroceramics	ZrO_2	10, 80
Electrode materials	Ni-Mo	81
Ferrites	Mn-Zn, Ni-Zn	82, 83
Ferroelectrics	$BaTiO_3$; $NaNbO_3$	84, 85
FGMs	Nb_5Si_3/Nb; Ti-Si-C	68, 86
Glassy materials	Fe-Co-Nd-Dy-B; Fe-Co-Ga-P-C-B	87, 88
Hard materials	WC, SiC, B_4C	89, 90, 65, 66
Intermetallics	$NbAl_3$; FeAl; NiTi	91, 92, 93
Joining of materials	Mo/$CoSb_3$	94, 95
Laminates	SiC/TiC; Si_3N_4-SiC/BN-Al_2O_3	96, 97
Machinable ceramics	Si_3N_4/BN; Al_2O_3/Ti_3SiC_2	98, 99
Magnetic	Nd-Fe-B; Nd-Fe-Co-V-B	100, 101
Nanostructures	ZrO_2; Ti-Al-B	10, 102
Nanotubes	Carbon	103, 104
Phosphors	ZnS family	105
Piezoelectrics	K-Na niobate; Sr-Ca-Na niobate	106, 107
Porous materials	Al; $FeSi_2$	108, 109
Pyroelectrics	Pb zirconate-Pb titanate-Pb	110
Shape memory materials	Cu-Zn-Al; NiTi	111, 112
Solid solutions	TiB_2-WB_2-CrB_2; TiB_2-WB_2	113, 114
Sputter targets	In-Sn oxide; Pb titanate	115, 116
Superconductors	MgB_2; Nb_3Al	117, 118
Synroc	Titanate ceramics	119
Thermoelectric	$(Bi,Sb)_2Te_3$; Mg_2Si	120, 121
Transparent ceramics	MgO; AlN	122, 123

process has been used to simultaneously synthesize and densify nanostructured ceramic, intermetallic and composite materials in bulk form [61–66]. It has also been used to microalloy ceramics for ductility improvement [67], and to form functionally-graded materials [68]. The above references serve only as examples of a large number of investigations published on the use of the SPS method. As was mentioned at the beginning of this review, our intent is not to discuss all published papers but to provide a review on those which dealt with fundamental issues concerning field activation in general and the SPS method in more defined terms. However, to make this review useful to those interested in specific applications, we provide in Table I a summary of research activities utilizing the SPS with a specific material designation. In view of the large number of publications, the papers referenced in Table I represent, per force, only selected examples from the recent literature.

In most of the published accounts, it has been variously concluded that the SPS process produced materials with decidedly improved properties. Improvements in mechanical properties [124, 125], oxidation and corrosion resistance [125, 127], optical transmission [128], microstructure [129, 130], and electrical properties [53, 131] have been reported. An attempt to critically evaluate these results is difficult since it is not possible to separate the effect of density and temperature from any intrinsic effect of the process. In nearly all investigations using the SPS method it is reported that higher densities and lower sintering temperatures are achieved. The high density and the concomitant smaller grain size have a direct effect on nearly all properties investigated on the sintered materials. Thus it is likely that many of the claims of superiority of the method are likely to be related to these microstructural considerations. In stating this, however, it not intended to conclude that other, intrinsic effects are not operative. A discussion of these with specific reference to the SPS process will be given below.

4. Characteristics of the process

The SPS process involves the sintering of powders under the simultaneous influence of a current and pressure. Powders are placed in a die (typically graphite) and heating is effected by passing a current (typically pulsed DC) through the die and the sample (if the latter is conducting) while a pressure is applied on the powder. The characteristics, therefore, include (a) high heating rate, (b) the application of a pressure, and (c) the effect of the current. While similar in some aspects to hot-pressing, the SPS process is typically characterized by a higher heating rate and the application of the current. In what follows we will examine these parameters and discuss their role in the success of this process as a method to sinter or reaction-sinter materials.

4.1. Effect of heating rate

One of the significant differences between the conventional hot-pressing and SPS methods is the heating rate. In the latter heating rates as high as 1000°C/min can be achieved. This feature of the SPS method is related to the way in which the sample and the die are heated, as will be discussed below.

The effect of heating rate on sintering has been investigated considerably in both pressureless and pressure-assisted sintering. In pressureless sintering, higher heating rates have been shown to enhance densification by by-passing the non-densifying mechanism of surface diffusion and by creating an additional driving force due to large thermal gradients [24]. The objective is to suppress particle coarsening and enhance particle sintering. Investigations on the effect of heating rate on densification and grain growth in the SPS have produced conflicting results, however. In the sintering of Al_2O_3 (a non-conductor) and

$MoSi_2$ (a reasonably good conductor), it was found that heating rate (between 50 and 700°C/min) had no effect on the final density for samples sintered at the same temperature and for the same hold time [132]. The grain size of alumina showed a dependence on heating rate (had an inverse relationship with heating rate) but that of $MoSi_2$ had no dependence on heating rate. In contrast to these observations, the work of Shen *et al.* [133] on alumina showed that heating rate had little effect on the density up to a value of about 350°C/min and then had a negative effect on the final density with higher heating rates (the density decreased as the rate increased up to 600°C/min). The grain size, however, showed a dependence which was strongest for lower heating rates (the grain size decrease was significant as the heating rate increased fro 50 to 200°C/min). In a more recent study by Zhou *et al.* [134], it was shown that heating rate in the range 50–300°C/min had no marked influence on the final density of alumina but had a significant effect on the grain size (grain size decreased with increasing heating rate).

In our recent work on the densification of nanometric fully-stabilized cubic zirconia [10], we observed similar effects: no dependence of the final density on heating rate, but a similar dependence of grain size for rates ranging from 50 to 300°C/min. In an earlier conventional sintering study, Chen and Mayo [135] investigated the effect of heating rate of partially-stabilized (3 mol% yttria) zirconia with two different particle sizes. For submicrometer sized powders, the final density showed no dependence on heating rate but for nanometric powders an increase in heating rate resulted in a decrease in the final density. The authors explained this latter observation on the basis of large thermal gradients existing with high heating rates. These in turn cause the outside of the sample to sinter while the inside still has considerable porosity. This point leads us to focus on the accuracy of temperature measurements in typical SPS experiments. The different observations are, in part, due to uncertainty in temperature measurements since in most cases this parameter is measured pyrometrically on the surface of the graphite die [136].

4.2. Effect of applied pressure

When powders are sintered under an applied pressure, higher densification is achieved at the same temperature. There are numerous examples based on the use of hot-pressing investigations [137]. The pressure has a mechanical role as well as an intrinsic role. Mechanically the pressure has a direct effect on particle re-arrangement and the destruction of agglomerates, particularly in the case of nanometric powders. The intrinsic effect of the pressure can be assessed from the driving force for sintering:

$$\frac{d\rho}{(1-\rho)dt} = B\left(g\frac{\gamma}{x} + P\right) \tag{2}$$

where ρ is the fractional density, B is a term that includes diffusion coefficient and temperature, g is a geometric constant, γ is the surface energy, x is parameter that represent a size scale (an hence is related to particle size), t is time, and P is the applied external pressure. The first term on the RH side of Equuation 2 represents the intrinsic driving force for sintering while the second term represents the intrinsic contribution to the driving force by the applied pressure. The significance of the pressure on sintering thus depends on the relative magnitudes of the two terms. When the particle size (related to γ) is small, the relative contribution of the pressure is small, but becomes significant as the particle size increases. The point at which the two contributions are equal is represented by

$$P = g(\gamma/x) \tag{3}$$

Equation 3 provides the determination of the critical particle size above which the contribution of the pressure to the densification driving force becomes dominant. In a study on the sintering of nanometric pure zirconia, Skandan *et al.* [138] found that the pressure had no effect on the relative density of fine-grained powder (6 nm) up to a pressure of about 35 MPa, but the density increased sharply when higher pressure was used. For larger particle size powder (12 nm), the same behavior was seen except that the transition occurred at about 10 MPa.

The influence of pressure can be examined at a more fundamental level. Under a stress, the chemical potential, μ_I, at a particle interface is modified such that [139],

$$\mu_I = \mu_i^0 - \sigma_n \Omega_I \tag{4}$$

where $\mu^0{}_i$ is the reference (or standard) chemical potential, σ_n is the normal stress at the interface, and Ω_I is the atomic volume of the diffusing species. In Equation 4 a tensile stress is positive while a compressive stress is negative. Incorporating electric fields induced by space charge in ionic materials, Raj and co-workers [139, 140] modified the above relationship such that

$$\mu_I' = \mu_i^0 - \sigma_n \Omega_I + ez\phi \tag{5}$$

where $\mu_I{}'$ is now the electrochemical potential, e is the electron charge, z is the valence of the diffusing ion, and ϕ is the local electric potential. The validity of Equation 5 was demonstrated by Pannikkat and Raj [140] by measuring a potential difference on two faces of zirconia samples, one subjected to stress while the other was stress-free. This consideration has implications in SPS sintering of ionic materials and it has not received any attention to the best of our knowledge.

The above discussion can be summarized in terms of an increased driving force for sintering as a result of the

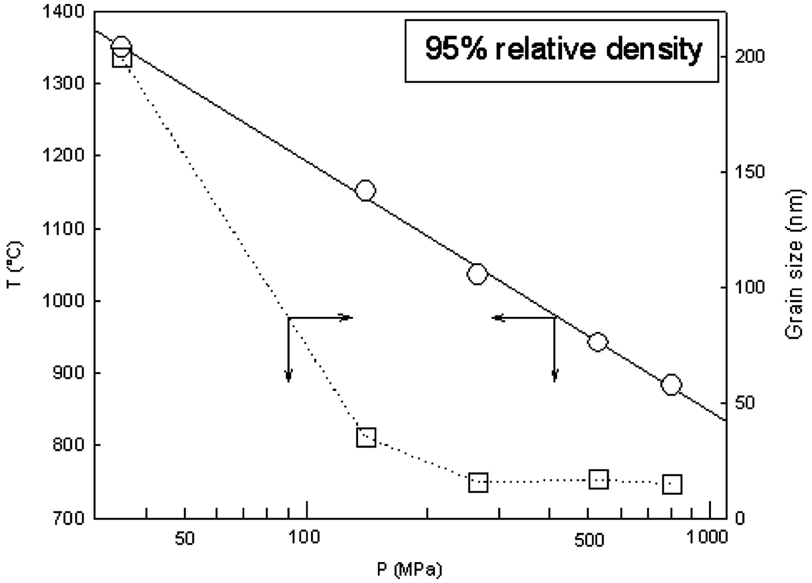

Figure 6 Effect of pressure on the temperature needed to get 95% relative density for cubic ZrO_2. The corresponding decrease in grain size is also shown.

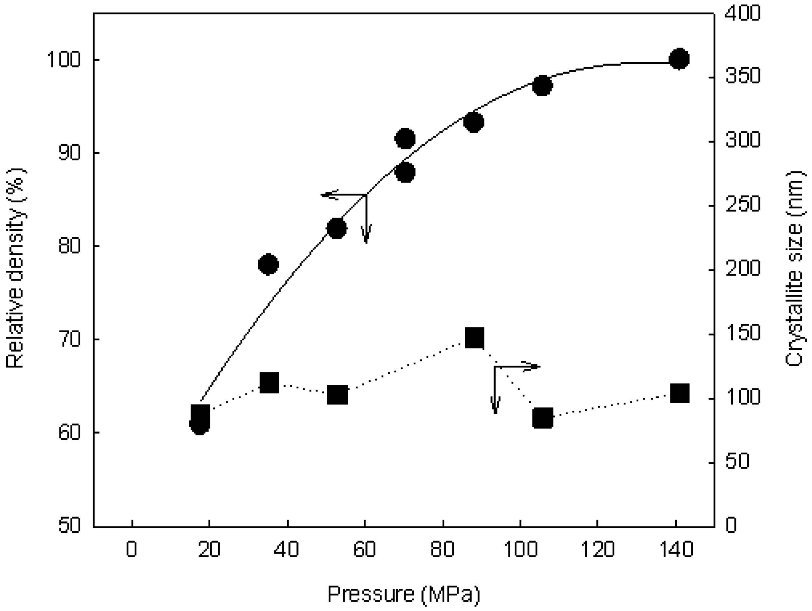

Figure 7 The effect of applied pressure on the density and grain size of cubic ZrO_2. Constant temperature of 1200°C, hold time 5 min, heating rate 200°C/min.

application of a pressure. This leads to a decrease in the sintering temperature and a limitation of grain growth. Validation of this conclusion has been provided in many of the recent SPS investigations. Fig. 6 shows the effect of pressure on the sintering temperature required to obtain a 95% relative density of nanometric cubic zirconia (with 5 min hold time) sintered in an SPS apparatus [23]. The figure also shows grain size obtained under these conditions. The temperature required to achieve the 95% density decreases linearly with the logarithm of the applied pressure. The grain size decreased from about 200 to 15 nm. The effect of pressure on density and grain size when sintering was carried out at constant temperature is shown in Fig. 7 for another powder of cubic zirconia [10]. It is seen that while the pressure has no effect on the grain size, it has a marked influence on the density after sintering for 5 min at 1200°C.

4.3. Role of the current

As pointed out above the major difference between convention hot-pressing and the SPS methods relates to differences in heating rate, which are in turn due to the methods in which the sample and the die are heated in the two cases. Typically, in hot-pressing the sample (and the die) is heated by radiation from an enclosing furnace. In contrast, in the SPS method the die (typically graphite) and sample are heated by Joule heating from a current passing thorough them (if the sample is conducting). However, in addition to providing heat, the current (typically pulsed DC current) has been assigned another role: that of creating plasma. The plasma is proposed to cause a cleansing effect on the surface of the particles leading to sintering enhancement. This role of the current has been advocated by many [22, 133, 141, 142] and has been doubted by others for lack of unambiguous experimental evidence [143–145]. Tokita [146] has presented evidence for neck formation between particles because of plasma. However, this evidence has been described as not convincing by others [144]. On the other hand, in an investigation on the sintering of Al powders by SPS Ozaki *et al.* [147] concluded that no discharge was present when the conducting graphite die was used. With regard to the role of plasma, the recent work of Yanagisawa *et al.* [148] is worth noting. Copper powder particles were subjected to single-pulse discharges (500 ms duration) and the authors observed that sparks could form between some but not all particles. However, the important observation was that the neck formation occurred in both cases with no apparent advantage of spark formation.

The existence of plasma (discharge) must be evaluated with other considerations. These include the role of applied pressure and the stage of sintering. Both of these parameters relate to the formation of large contact areas between the particles. While initially, a discharge may be possible in conducting powders, as contacts between particles increase (because of sintering or the applied pressure), the likelihood of discharge becomes small. This issue becomes further complicated when one examines the sintering of non-conducting powders, e.g., alumina. Makino's work on the sintering of Al_2O_3 showed that only a small current (about 100 mA) can pass through the sample at 1000°C, which is relatively insignificant when compared with the total current (about 1000 A) [149]. In a similar study, Tomino *et al.* [150] concluded that no current passed through the alumina samples and thus these findings seem to rule out the generation of discharge within the non-conducting sample.

4.3.1. Effect of pulsing

An important aspect of the current application in the SPS is the pulsing and its proposed effect on the creation of the plasma and hence its influence on the sintering behavior. Two recent publications on the effect of pulsing are worth noting here. Xie *et al.* [145] investigated the effect of the frequency of pulsing on the sintering of aluminum. They sintered samples at pulse frequencies of 10, 40, and 300 kHz and also with DC current (0 Hz) and found no effect on relative density, electrical resistivity, and tensile properties of the sintered material.

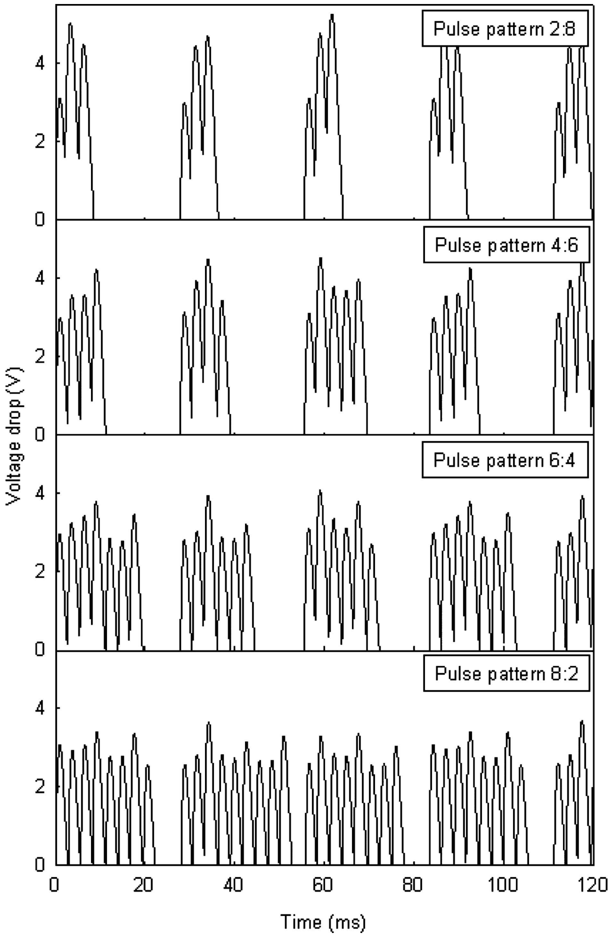

Figure 8 SPS pulse patterns for various on:off settings.

In a more recent investigation, Chen *et al.* [44] investigated the effect of pulsing on the reaction and product formation between layers of Mo and Si in the SPS. Pulse waveforms generated in the SPS (Sumitomo, Model 1050), depicted in Fig. 8, show that the voltages are not constant for all pulses and in some cases, the number of pulses is not the same as the set value (for example the 2:8 pattern contains 3 on pulses rather than 2). As the pattern changes with more off than on pulses (e.g., from 8:2 to 2:8), the amplitude of the voltage of the pulse increases to compensate for the power requirement under constant temperature control, Fig. 9. Fig. 10 shows that the RMS value of the current remains constant regardless of the change in pulse pattern, an observation consistent with the fact that the RMS value is indicative of the dissipated power which must be constant if the temperature of the sample is to remain constant fr all these patterns. In order to evaluate the effect of pulsing pattern on mass transport in the SPS, Chen *et al.* [44] examined the reactivity between layers of Mo and Si since such a geometry leads to easier interpretation of the sought after effect. The results

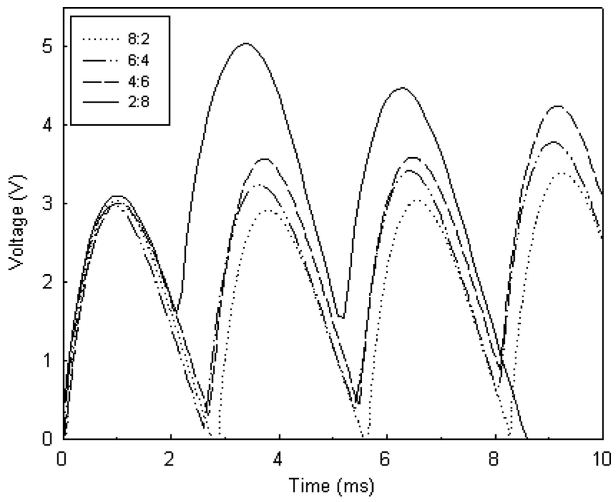

Figure 9 Effect of pulse pattern on voltage amplitude in the SPS.

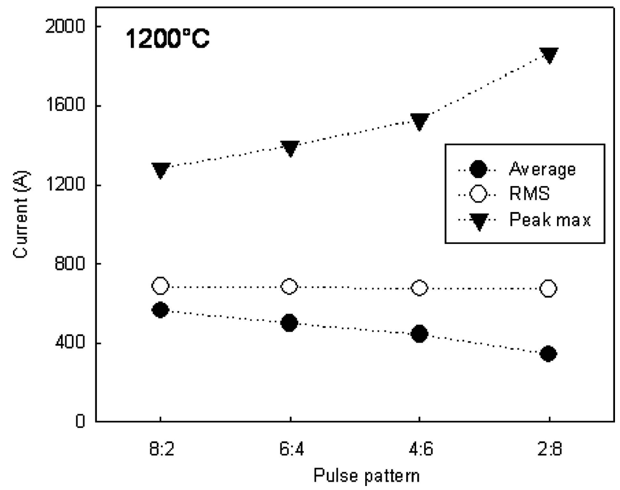

Figure 10 Changes in peak, average and RMS values of the current with pulse pattern in the SPS.

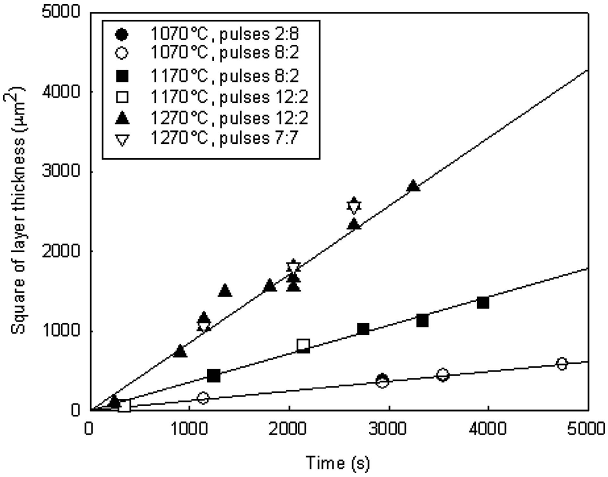

Figure 11 The effect of pulse pattern on the growth of $MoSi_2$ at different temperature in the SPS.

showed that the thickness of the product layer (primarily $MoSi_2$) was independent of the direction of the current (or the electrons); the thickness was the same regardless if the electrons flowed from Si to Mo or the opposite. More important, however, is the observation that the thickness of the product was independent of the pulse pattern, as can be seen from Fig. 11.

4.3.2. Effect of the current on mass transport

As was pointed out in a previous section of this review, the application of a current has an influence on mass transport. The influence can be manifested through the electron wind effect (electromigration) [46], or by an increase in point defect [48], or by a decrease in the activation of migration of the defects [49]. The determination of this intrinsic influence must be isolated from the Joule heating accompanying the passage of the current as has been done in our recent investigations [41–43, 47]. However, in the SPS, the current and temperature are dependent variables and their influence cannot be clearly separated. Nevertheless, we have conducted experiments in the SPS to determine the effect of the current on mass transport involved in the reaction between Mo and Si [136]. The sample was again in the form of a three layer ensemble: an Si wafer between two Mo foils. In such experiments it is crucial that the temperature of the sample is measured accurately which was accomplished by a thermocouple in contact with the bottom of the sample. For the case of reactivity with a current, no die was used and the current flowed through the sample assembly only. And for reactivity without a current, the sample was placed in a die but was electrically isolated by two alumina wafers placed at the top and bottom of the sample assembly.

When the reaction between Si and Mo was carried out under the influence of a current, products (primarily $MoSi_2$ with minor amounts of Mo_5Si_3) formed at the two Mo/Si interfaces representing two different directions of the electrons (from Si to Mo and from Mo to Si). As Fig. 12 shows, there is no difference in the thickness of the product layer at both interfaces. In the classical electromigration experiments a dependence on the current direction is anticipated, but in those cases the diffusion is in dilute solutions without the complication of phase formation and its diffusional requirements as has been discussed elsewhere [42]. What is more important, however, is the observation that the current (under a constant pulse pattern of 12:2) had a significant influence on the reaction between Mo and Si in the SPS, as can be seen in Fig. 13. A kinetic analysis of the rate of growth of the product with and without a

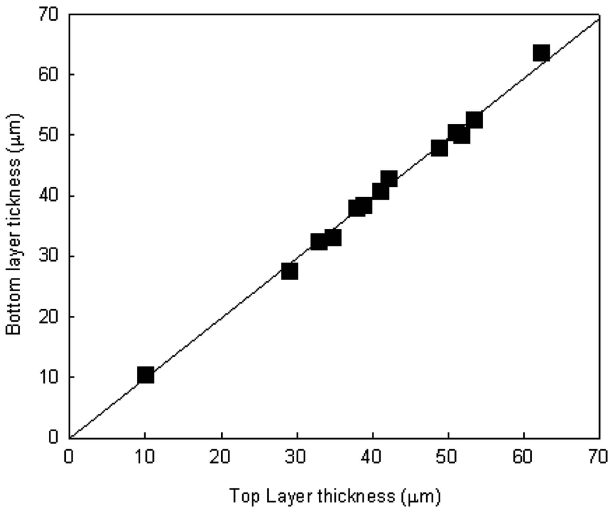

Figure 12 Comparison between $MoSi_2$ layer thickness at the two (Mo-Si and Si-Mo) interfaces relative to the direction of the current.

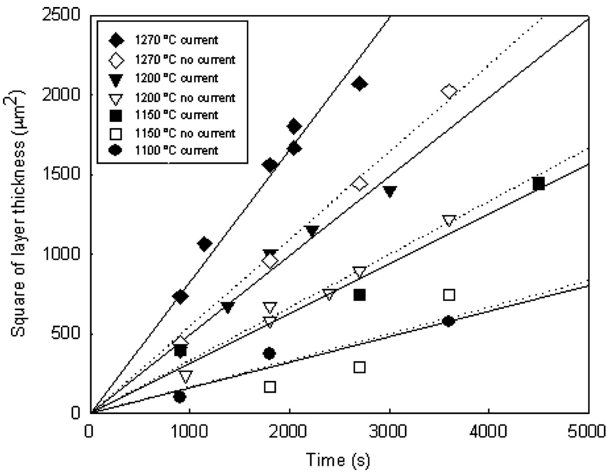

Figure 13 Growth rates of the $MoSi_2$ layer at different temperatures in presence and absence of current.

current gave approximately the same activation energy (168 vs. 175 kJ/mol with and without a current, respectively), implying that the mechanism of formation of the product phase was not altered by the current. Thus it is likely that the enhanced mass transport is due to a change in defect concentration or enhanced mobility of the defects.

5. Modeling study on the SPS process

Relatively few attempts have been made to simulate the SPS process and gain insight on the effect of its various parameters. In all of these, however, the role of the current has been restricted to Joule heating. The early attempts to simulate the effect of a current on the reaction between powders in a compact focused on the kinetics and dynamics of the reaction front [151]. In that study, which did not include the die in the simulation, it was shown that the assumed volume combustion (where the reaction between powders takes place simultaneously over the entire sample is not valid for all conditions, but depended on the nature of the material and the size of the sample. Waveform reactions occurred when samples of larger diameter were used. More recent simulation studies have accounted for the die and in this regard are more closely relate to the conditions of the SPS [152–154]. Heian *et al.* [154] simulated the conditions under which a composite of $MoSi_2$/SiC is synthesized from the elements in the SPS. Again the model assumed the contribution of the current to be only thermal (Joule heating) and it did not account for the role of the pressure. The results showed the sequence of phase formation and the shape of the reaction front and their dependence on sample size. Fig. 14a and b show the time dependence of the profiles of temperature, current, conversion of $MoSi_2$, and conversion of SiC for samples with radii of 1 and 4 cm, respectively. In these figures the thickness of the graphite die is 1 cm for both cases. It can be seen that for the smaller sample the combustion reaction is of the volume type for both components (i.e., takes place simultaneously throughout the sample). In contrast the combustion reaction is of the waveform for both when the sample is larger. The significance of this relates to the fact that waveform combustion is associated with large temperature gradients and hence an influence on microstructure. The effect of sample and die conductivity on the process of formation of the composite in the SPS was also evaluated in this modeling study [154].

The temperature and current distribution in the SPS was modeled recently for conducting (copper) and non-conducting (alumina) samples [155]. Current density distributions for these cases in the vertical and radial directions are shown in Figs. 15 and 16, respectively. As anticipated, the non-conducting sample does not carry any current, an obvious observation with significant implication in the concept of plasma or discharge in the SPS, as was pointed out above. In such a case, the sample is heated thermally from the die, as can be seen from Fig. 17 (the sample size is 19 mm diameter). The temperature within the sample does not become relatively uniform until after about 100 s of heating. Since modeling has shown that the highest current density (and hence temperature) is located in the punches of the die [155], the location of the sample along the vertical axis inside the die becomes important. Fig. 18 shows the difference in temperature between two faces of a 3 mm thick alumina sample as a function of displacement from the muddle point of the die. A displacement of 6 mm results in a ΔT of about 100°C. An experimental verification for the occurrence of such a temperature difference was provided by an investigation on the sintering

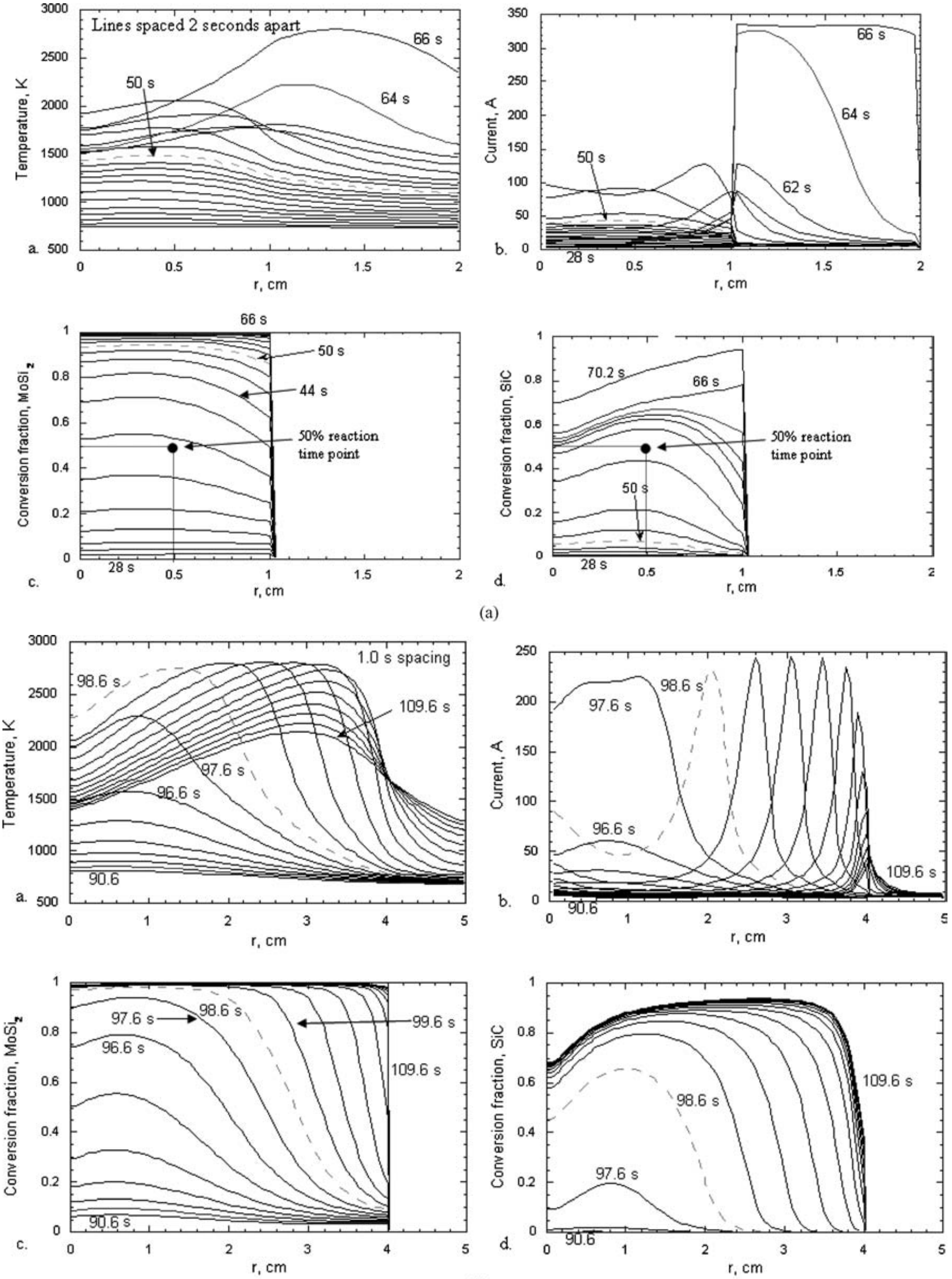

(a)

(b)

Figure 14 Modeling results of time dependence of profiles of temperature, current, conversion to MoSi$_2$, and conversion to SiC for SPS synthesis of MoSi$_2$/SiC composites: (a) sample radius=1 cm, and (b) sample radius=4 cm.

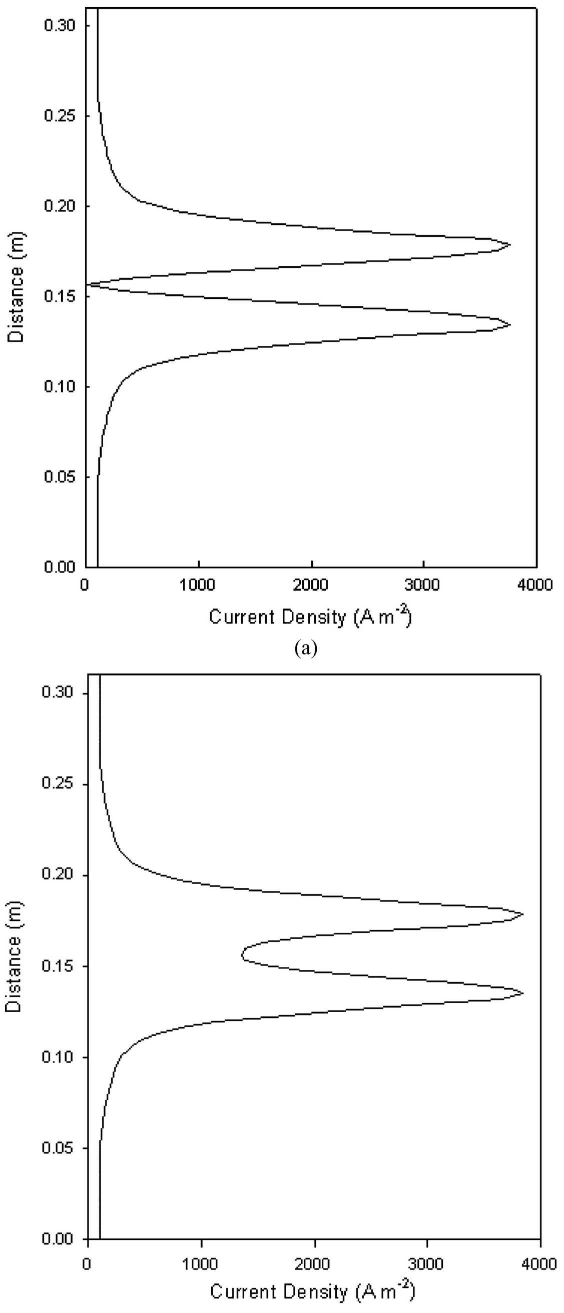

(a)

(b)

Figure 15 Current density distribution along the vertical (*z*-axis) of die and sample assembly in the SPS: (a) non-conducting (alumina) sample, and (b) conducting (copper) sample. Applied voltage=5 V.

of cubic zirconia. Fig. 19 shows a ZrO_2 sample sintered in at 1200°C with discoloration on one side [155]. The dark portion represents oxygen deficiency in the oxide as a result of the low partial pressure of oxygen in the SPS [10, 156]. This pressure is a function of temperature and the white portion of the sample saw a lower temperature.

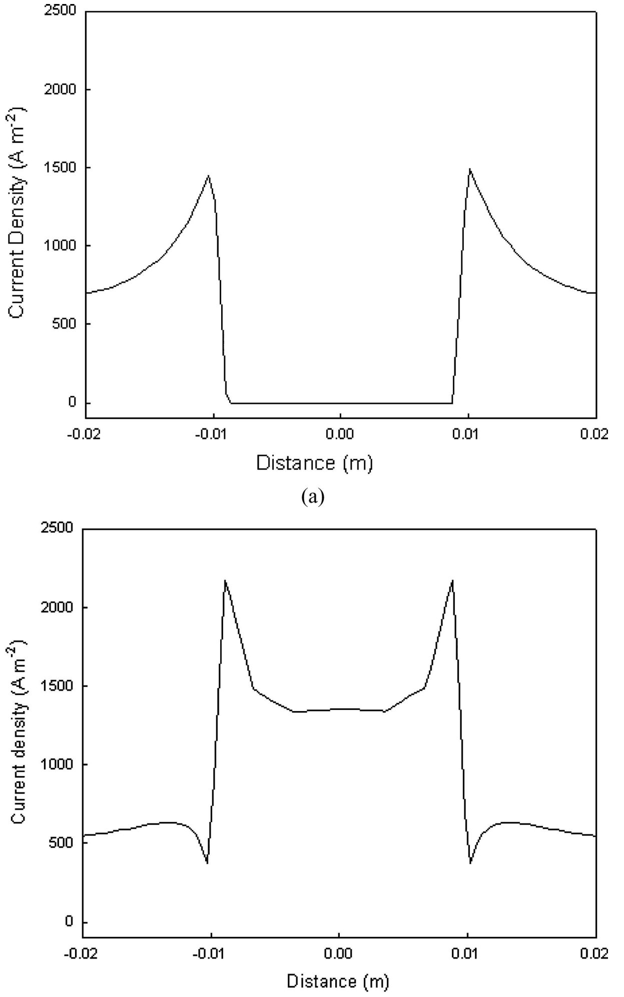

(a)

(b)

Figure 16 Radial distribution of current density for (a) alumina, and (c) copper. Applied voltage=5 V.

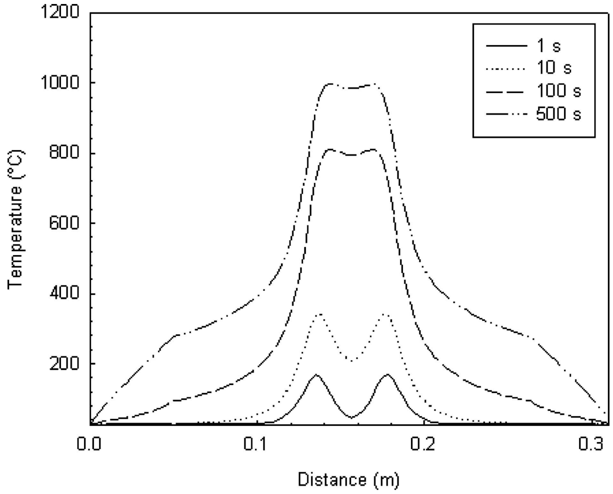

Figure 17 Calculated temperature distribution along vertical axis for different times after the application of current in the SPS. Alumina sample is 3 mm thick; applied voltage=4 V.

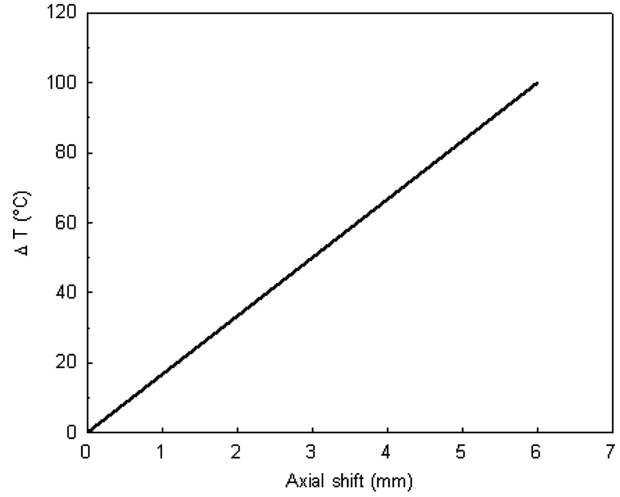

Figure 18 Calculated temperature differences between two faces of sample as a function of vertical displacement from center of die. Sample: 3 mm thick alumina; applied voltage=5 V.

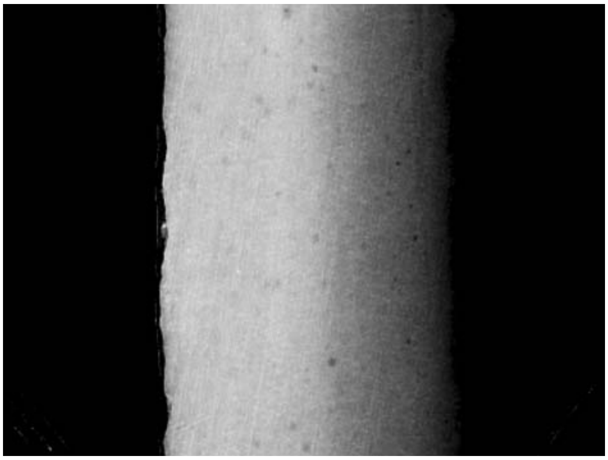

Figure 19 Discoloration gradient in nanometric zirconia sample sintered at 1200°C for 5 min under pressure of 106 MPa.

6. Concluding remarks

The use of a current or electric discharge to enhance sintering has been known for more than seven decades. The recent commercialization of the technique has resulted in the widespread use of this form of activated sintering, with more than 150 papers published per year recently. In most of these literature accounts a clear benefit of the method, relative to conventional consolidation techniques is demonstrated: higher density, smaller grain size, cleaner grain boundaries, and other attractive properties. The explanation generally advanced for these observations is the role of presumed plasma forming between particles in the sintering compacts.

The significant features of the spark plasma sintering (SPS) method include high heating rate, the application of pressure, and the effect of the current. An analysis of each of these parameters is provided, with emphasis on fundamental aspects. The intrinsic contributions of the current to mass transport have received little attention, but their role in SPS and non-SPS processes has been clearly demonstrated in recent investigations. While the role of plasma has been advocated, its existence in SPS experiments, particularly when non-conducting powders are used, has not been unambiguously demonstrated and remains an important objective of attempts to provide a clear understanding of the process. Such a fundamental investigation (and related research) would help avoid the creation of a "black box" stigma for the SPS by providing the physical underpinnings of the process.

Acknowledgements

We are grateful for the support of this work by the Army Research Office.

References

1. W. D. KINGERY, in "Sintering' 91," edited by A. C. D. Chaklader and J. A. Lund, (Trans Tech, Brookfield, VT, 1992) p. 1.
2. J. E. BURKE, *Ceramics and Civilization* **1** (1985) 315.
3. G. C. KUCZYNSKI, *Trans. AIME* **185** (1949) 169.
4. F. V. LENEL, *ibid.* **175** (1948) 878.
5. R. L. COBLE, *J. Amer. Ceram. Soc.* **41** (1958) 55.
6. W. D. KINGERY and M. BERG, *J. Appl. Phys.* **26** (1955) 1205.
7. R. M. GERMAN and Z. A. MUNIR, *Met. Trans* **6A** (1975) 2229.
8. *Idem.*, *J. Amer. Ceram. Soc.* **59** (1976) 379.
9. Z. A. MUNIR and R. M. GERMAN, *High Temp. Sci.* **9** (1977) 275.
10. U. ANSELMI-TAMBURINI, J. E. GARAY, Z. A. MUNIR, A. TACCA, F. MAGLIA and G. SPINOLO, *J. Mater. Res.* **19** (2004) 3255.
11. G. F. TAYLOR, US Patent No. 1,896,854, 1933.
12. *Idem.*, US Patent No. 1,896,853, 1933.
13. G. D. CREMER, US Patent No. 2,355,954, 1944.
14. V. F. LENEL, *Trans. AIME* **203** (1955) 158.
15. R. W. BOESEL, M. I. JACOBSON and I. S. YOSHIOKA, Proc. Fall Powder Met. Conf. Metal Powder Industries Federation, New York, pp. 75–99, 1970.
16. C. G. GOETZEL and V. S. DEMARCHI, *Powder Met. Int.* **3** (1971) 80.
17. K. INOUE, US Patent 3,340,052, 1967.
18. *Idem.*, US Patent 3,656,946, 1972.
19. I. J. SHON and Z. A. MUNIR, *Mater. Sci. Engin.* **A202** (1995) 256.
20. G. XIE, O. OHASHI, M. SONG, K. MITSUISHI and K. FURUYA, *Appl. Surf. Sci.* **241** (2005) 102.
21. W. M. GOLDBERGER B. MERKLE and D. BOSS, *Adv. Powder Metall. Particulate Mater* **6** (1994) 91.
22. M. TOKITA, *Mater. Sci. Forum* **308–311** (1999) 83.
23. U. ANSELMI-TAMBURINI, J. E. GARAY and Z. A. MUNIR, to be submitted, 2005.
24. R. M. GERMAN, Sintering Theory and Practice, (Wiley, New York, 1996) p. 482.
25. D. E. CLARK and W. H. SUTTON, *Ann. Rev. Mater. Sci.* **26** (1996) 299.
26. Z. A. MUNIR and H. SCHMALZRIED, *J. Mater Synth. Process.* **1** (1993) 3.
27. H. CONRAD (Ed.), *Mater Sci. Engin.* (special issue), **A287**(2) (2000) 190.

28. R. J. SCHWENSFEIR JR. and C. ELBAUM, *Phys. Chem. Solids* **26** (1965) 781.
29. Z. A. MUNIR and T. T. NGUYEN, *Phil. Mag.* **A47** (1983) 105.
30. Z. A. MUNIR and A. A. YEH, *ibid.* **A56** (1987) 63.
31. C. A. MACHIDA and Z. A. MUNIR, *J. Cryst. Growth,* **68** (1984) 665.
32. W. LIU and J. Z. CUI, *J. Mater. Sci. Lett.* **16** (1997) 1410.
33. *Idem., Scripta Metall Mater.* **33** (1995) 623.
34. H. CONRAD, *Mater. Sci. Eng.* **A287** (2000) 276.
35. M. ZHEN, X. P. LU and H. CONRAD, *Scripta Mater.* **44** (2001) 381.
36. K. JUNG and H. CONRAD, *J. Mater. Sci.* **39** (2004) 1803.
37. C. SCHALANSKY and Z. A. MUNIR *J. Cryst. Growth* **97** (1989) 310.
38. Z. A. MUNIR, *Zeit. Physik. Chem.,* **207** (1998) 39.
39. *Idem., Solid State Ionics,* **101** (1997) 991.
40. T. B. HOLLAND, J. F. LÖFFLER and Z. A. MUNIR, *J. Appl. Phys.* **95** (2004) 2896.
41. J. R. FRIEDMAN, J. E. GARAY, U. ANSELMI-TAMBURINI and Z. A. MUNIR, *Intermetallics* **12** (2004) 589.
42. J. E. GARAY, U. ANSELMI-TAMBURINI and Z. A. MUNIR, *Acta Mater.* **51** (2003) 4487.
43. N. BERTOLINO, J. GARAY, U. ANSELMI-TAMBURINI and Z. A. MUNIR, *Phil. Mag. B* **82** (2002) 969.
44. W. CHEN, U. ANSELMI-TAMBURINI, J. E. GARAY, J. R. GROZA and Z. A. MUNIR, *Mater. Sci. Eng* **A394** (2005) 132.
45. C. OETZEL, R. CLASEN and J. TABELLION, *Ceram. Forum Int.* **81** (2004) E35.
46. H. B. HUNTINGTON, in "Diffusion in Solids", edited by A. S. Nowick and J. J. Burton (Academic Press, New York, 1975) p. 306.
47. N. BERTOLINO, J. GARAY, U. ANSELMI-TAMBURINI and Z. A. MUNIR, *Scripta Mater.* **44** (2001) 737.
48. P. ASOKA-KUMAR, M. ALATALO, V. J. GOSH, A. C. KRUSEMAN, B. NIELSON and K. G. LYNN, *Phys. Rev. Lett.* **77** (1996) 2097.
49. J. E. GARAY, S. C. GLADE, U. ANSELMI-TAMBURINI, P. ASOKA-KUIMAR and Z. A. MUNIR, *Appl. Phys, Lett.* **85** (2004) 573.
50. V. MAMEDOV, *Powder Metall.* **45** (2002) 322.
51. Z. SHEN and M. NYGREN, *Key Eng. Mater.* **247** (2003) 79.
52. S. H. RISBUD, J. R. GROZA and M. J. KIM, *Phil. Mag. B* **69** (1994) 525.
53. X. J. CHEN, K. A. KHOR, S. H. CHAN and L. G. YU, *Mater. Sci. Eng.* **A374** (2004) 64.
54. Z. SHEN, H. PENG and M. NYGREN, *Adv. Mater.* **15** (2003) 1006.
55. T. TAKEUCHI, E. BETOURNE, M. TABUCHI, H. KAGEYAMA, Y. KOBAYASHI, A. COATS, F. MORRISON, D. C. SINCLAIR and A. R. WEST, *J. Mater. Sci.* **34** (1999) 917.
56. M. YUE, J. ZHANG, Y. XIAO, G. WANG and T. LI, *IEEE Trans Magnetics* **39** (2003) 3551.
57. N. ICHINOSE, *Ceram. Trans.* **74** (1997) 133.
58. H. FURUHASHI and O. OHHASHI, *J. Jpn. Instit. Metals* **67** (2003) 448.
59. D. KUSANO and Y. HORI, *ibid.* **66** (2002) 1063.
60. J. YAMAMOTO, Y. SHIMIZU, H. OHTANI, K. SHIOZAKI and K. SKAKAKI, *ibid.* **67** (2003) 555.
61. R. ORRU, J. WOOLMAN, G. CAO and Z. A. MUNIR, *J. Mater. Res.* **16** (2001) 1439.
62. F. BERNARD, F. CHARLOT, E. GAFFET and Z. A. MUNIR, *J. Amer. Ceram. Soc.* **84** (2001) 910.
63. J. W. LEE, Z. A. MUNIR, M. SHIBUYA and M. OHYANAGI, *ibid.* **84** (2001) 1209.
64. T. YAMAMOTO, H. KITAURA, Y. KODERA, T. ISHII, M. OHYANAGI and Z. A. MUNIR, *ibid.* **87** (2004) 1436.
65. M. OHYANAGI, T. YAMAMOTO, H. KITAURA, Y. KODERA, T. ISHII and Z. A. MUNIR, *Scripta Mater.* **50** (2004) 111.
66. E. M. HEIAN, S. K. KHALSA, J. W. LEE, Z. A. MUNIR, T. YAMAMOTO and M. OHYANAGI, *J. Amer. Ceram. Soc.* 87 (2004) 779.
67. J. N. WOOLMAN, J. J. PETROVIC and Z. A. MUNIR, *Scripta Mater.,* **48** (2003) 819.
68. E. M. HEIAN, J. C. GIBELING and Z. A. MUNIR, *Mater. Sci. Eng.* **A368** (2004) 168.
69. M. OSKARSSON, P. LUNDBERG, A. PETTERSSON, P. PETTERSSON and M. NYGREN, Proc. 20th Int. Sympos. Ballistics, 2002, p. 1182.
70. Y. GU, K. A. KHOR and P. CHEANG, *Biomater.* **25** (2004) 4127.
71. A. NAKAHIRA, M. TAMAI, H. ARITANI, S. NAKAMURA and K. YAMASHITA, *J. Biomed. Mater. Res.* **62** (2002) 550.
72. S. D. DE LA TORRE, D. OLESZAK, A. KAKITSUJI, K. MIYAMOTO and H. MIYAMOTO, *Mater. Sci. Eng. A* **A276** (2000) 226.
73. Z. SONG, S. KISHIMOTO and N. SHINYA, *J. Mater. Sci.* **38** (2003) 4211.
74. H. C. KIM, I. J. SHON and Z. A. MUNIR, *ibid.* in press (2005).
75. S. I. CHA, S. H. HONG and B. K. KIM, *Mater. Sci. Eng.* **A351** (2003) 31.
76. J. W. LEE, Z. A. MUNIR and M. OHYANAGI, *ibid.* **A325** (2002) 221.
77. X. Y. ZHANG, S. H. TAN and D. L. JIANG, *Ceram. Int.* **31** (2005) 267.
78. C. SHEN Q. F. LIU and Q. LIU, *Mater. Lett.* **58** (2004) 2302.
79. Y. GUO, K. KAKIMOTO and H. OHSATO, *Jap. J. Appl. Phys.* **42** (2003) 7410.
80. M. OKAMOTO, Y. AKIMUNE, K. FURUYA and M. HATANO, *Solid State Ionics* **176** (2005) 675.
81. S. D. DE LA TORRE, D. OLESZAK, F. ALMERAYA, A. MARTINEZ and R. MARTINEZ, *Mater. Sci. Forum* **343–346**(2) (2000) 855.
82. S. YAMAMOTO, S. HORIE, N. TANAMACHI, H. KURISU and M. MATSUURA, *J. Magnetism. Magnet. Mater.* **235** (2001) 218.
83. J. SUN, J. LI, G. SUN and W. QU, *Ceram. Int.* **28** (2002) 855.
84. M. T. BUSCAGLIA, V. BUSCAGLIA, M. VIVIANI, J. PETZELT, M. SAVINOV and L. MITOSERIU, *Nanotechnol.* **15** (2004) 1113.
85. T. WADA, K. TSUJI, T. SAITO, M. TAKEHISA and Y. MATSUO, *Jpn J. Appl. Phys.* **42** (2003) 6110.
86. Y. LUO, P. WEI, S. LI, R. WANG and J. LI, *Mater. Sci. Eng.* **A345** (2003) 99.
87. S. ISHIHARA, W. ZHANG, H. KIMURA, M. OMORI and A. INOUE, *Mater. Trans JIM.* **44** (2003) 138.
88. B. SHEN, H. KIMURA, A. INOUE, M. OMORI and A. OKUBO, *ibid.* **43** (2002) 1961.
89. H. C. KIM, I. J. SHON, J. E. GARAY and Z. A. MUNIR, *Int. J. Refractory Metals and Hard Materials* **22** (2004) 257.
90. S. CHA and S. H. HONG, *Mater. Sci. Eng* **A356** (2003) 381.
91. V. GAUTHIER, F. BERNARD, E. GAFFET, Z. A. MUNIR and J. P. LARPIN, *Intermetallics* **9** (2001) 571.
92. F. BERNARD, F. CHARLOT, E. GAFFET and Z. A. MUNIR, *J. Amer. Ceram. Soc.* 84 (2001) 910.
93. A. M. LOCCI, R. ORRÙ, G. CAO and Z. A. MUNIR, *Intermetallics* **11** (2003) 555.
94. J. FAN, L. CHEN, S. BAI and X. SHI, *Mater. Lett.* **58** (2004) 3876.
95. W. LIU and M. NAKA, *Scripta Mater.* **48** (2003) 1225.

96. C. YOU, D. JIANG and S. TAN, *J. Amer. Ceram. Soc.* **87** (2004) 759.
97. C. LI, Y. HUANG, C. WANG, K. TANG, S. LI and Q. ZAN, *Mater. Lett.* **57** (2002) 336.
98. W. S. CHO, J. H. LEE, M. W. CHO, E. S. LEE, D. S. PARK and Z. A. MUNIR, *Key Eng. Mater.* **287** (2005) 340.
99. Y. LUO, S. LI, W. PAN, J. CHEN and R. WANG, *J. Mater. Sci.* **39** (2004) 3137.
100. T. SAITO, T. TAKEUCHI and H. KAGEYAMA, *J. Mater. Res.* **19** (2004) 2730.
101. H. ONO, T. TAYU, N. WAKI, T. SUGIYAMA, M. SHIMADA, M. KANOU, A. FUJIKI, H. YAMAMOTO and M. TANI, *IEEE Trans. Magnetics* **39** (2003) 2081.
102. H. B. LEE, S. H. KIM, S. W. KANG and Y. H. HAN, *British Ceram. Trans.* **102** (2003) 231.
103. C. BALAZSI, Z. SHEN, Z. KONYA, Z. KASZTOVSKY, F. WEBER, Z. VERTESY, L. P. BIRO, I. KIRICSI and P. ARATO, *Composite Sci. Technol.* **65** (2005) 727.
104. G. D. ZHAN, J. D. KUNTZ, H. WANG and A. K. MUKHERJEE, *Therm. Conduct.* **27** (2005) 103.
105. N. KUBOTA, M. KATAGIRI, K. KAMIJO and H. NANTO, *Nucl. Instr. Methods Phys. Res.* **529** (2004) 321.
106. R. WANG, R. XIE, T. SEKIYA and Y. SHIMOJO, *Mater. Res. Bull.* **39** (2004) 1709.
107. R. J. XIE, Y. AKIMUNE, R. WANG, N. HIROSAKI and T. NISHIMURA, *Jpn. J. Appl. Phys.* **42** (2003) 7404.
108. C. E. WEN, M. MABUCHI, Y. YAMADA, K. SHIMOJIMA, Y. CHINO, H. HOSOKAWA and T. ASAHINA, *Mater. Sci. Forum* **426–432** (2003) 417.
109. F. KATSUKI, T. TOMIDA, A. TAKATA, K. YANAGIMOTO and S. MATSUDA, *Mater. Trans JIM* **41** (2000) 624.
110. Y. J. WU, N. UEKAWA, K. KAKEGAWA and Y. SASAKI, *Key Eng, Mater.* **228–229** (2002) 3.
111. N. J. PARK, S. J. LEE, I. S. LEE, K. S. CHO and S. J. KIM, *Mater. Sci. Forum,* **449–452** (2004) 1109.
112. T. WEISSGAERBER, N. REINFRIED, A. BOEHM and B. KIEBACK, *Adv. Powder Metall. Particulate Mater.* (Computer Opt. Disk) (2003) 980.
113. H. KAGA, E. M. HEIAN, Z. A. MUNIR, C. SCHMALZRIED and R. TELLE, *J. Amer. Ceram. Soc.* **84** (2001) 2764.
114. M. SHIBUYA, M. KAWATA, M. OHYANAGI and Z. A. MUNIR, *ibid.* **86**, (2003) 706–710.
115. T. TAKEUCHI, T. ISHIDA, K. ICHIKAWA, S. MIYAMOTO, M. KAWAHARA and H. KAGEYAMA, *J. Matter. Sci. Lett.* **21** (2002) 855.
116. T. TAKEUCHI, M. TAKAHASHI, K. ADO, N. TAMARI, K. ICHIKAWA and S. MIYAMOTO, *J. Amer. Ceram. Soc.* **84** (2001) 2521.
117. S. Y. LEE, S. I. YOO, Y. W. KIM, N. M. HEANG and Y. D. KIM, *ibid.* **86** (2003) 1800.
118. X. LI, A. CHIBA, M. SATO and S. TAKASHASH, *J. Alloys Compounds* **336** (2002) 232.
119. M. W. A. STEWART, M. L. CARTER, S. MORICCA, D. S. PERARA and E. R. VANCE, *J. Austral. Ceram. Soc.* **33** (1997) 43.
120. J. JIANG, L. CHEN, S. BAI, Q. YAO and Q. WANG, *Scripta Mater* 52 (2005) 347.
121. N. ARITA, K. KOGA, K. AKAI, H. KURISU, S. YAMAMOTO and M. MATSUURA, *Trans Mater. Res. Jpn.* **29** (2004) 2555.
122. R. CHAIM, Z. SHEN and M. NYGREN, *J. Mater. Res.* **19** (2004) 2527.
123. Z. Y. FU, J. F. LIU, H. WANG, D. H. HE and Q. J. ZHANG, *Mater. Sci. Technol.* **20** (2004) 1097.
124. M. NYGREN and Z. SHEN, *Silicates Industr.* **69** (2004) 211.
125. B. BASU, J. H. LEE and D. Y. KIM, *J. Amer. Ceram. Soc.* **87** (2004) 1771.
126. J. KUCHINO, K. KUROKAWA, T. SHIBAYAMA and H. TAKAHASHI, *Vacuum* **73** (2004) 623.
127. M. YUE, J. X. ZHANG, W. Q. LIU and G. P. WANG, *J. Magnetism Magnet. Mater.* **271** (2004) 364.
128. X. SU, P. WANG, W. CHEN, Z. SHEN, M. NYGREN, Y. CHENG and D. YAN, *J. Mater. Sci.,* **39** (2004) 6257.
129. Y. H. HAN, M. NAGATA, N. UEKAWA and K. KAKEGAWA, *British Ceram. Trans.* **103** (2004) 219.
130. Y. S. KWON, D. V. DUDINA, M. A. KORCHAGIN and O. I. LOMOVSKY, *J. Mater. Sci.* 39 (2004) 5325.
131. L. ZHOU, Z. ZHAO, A. ZIMMERMANN, F. ALDINGER and M. NYGREN, *J. Amer. Ceram. Soc.* **87** (2004) 606.
132. L. A. STANCIU, V. Y. KODASH and J. R. GROZA, *Metall. Mater. Trans. A* **32A** (2001) 2633.
133. Z. SHEN, M. JOHNSSON, Z. ZHAO and M. NYGREN, *J. Amer. Ceram. Soc.* **85** (2002) 1921.
134. Y. ZHOU, K. HIRAO, Y. YAMAUCHI and S. KANSAKI, *Scripta Mater.* **48** (2003) 1631.
135. D. J. CHEN and M. J. MAYO, *J. Amer. Ceram. Soc.* **79** (1996) 906.
136. U. ANSELMI-TAMBURINI, J. E. GARAY and Z. A. MUNIR, *Mater. Sci. Eng.* in press, 2005.
137. Ref. 24, p. 170.
138. G. SKANDAN, H. HAHN, B. H. KEAR, M. RODDY and W. R. CANNON, *Mater. Lett.* **20** (1994) 305.
139. J. JAMNIK and R. RAJ, *J. Amer. Ceram. Soc.* **79** (1996) 193.
140. A. K. PANNIKKAT and R. RAJ, *Acta Mater.* **47** (1999) 3423.
141. M. OMORI, *Mater. Sci. Eng.* **A287** (2000) 183.
142. D. ZHANG, Z. FU, R. YUAN and J. GUO, in Multiphased Ceramic Materials, edited by W. H. Tuan and J. K. Guo (Springer, Berlin, 2004) p. 65.
143. M. NYGREN and Z. SHEN, *Solid State Sci.* **5** (2003) 125.
144. S. W. WANG, L. D. CHEN, T. HIRAI and Y. S. KANG, *J. Mater. Sci. Lett.* **18** (1999) 1119.
145. G. XIE, O. OHASHI, K. CHIBA, N. YAMAGUCHI, M. SONG, K. FURUYA and T. NODA, *Mater. Sci. Eng.* **A359** (2003) 384.
146. M. TOKITA, *New Ceramics* **7** (1994) 63.
147. K. OZAKI, K. KOBAYASHI, T. NISHIO, A. MATSUMOTO and A. SUGIYAMA, *J. Jpn. Soc. Powder Metall.* **47** (2000) 293.
148. O. YANAGISAWA, H. KURAMOTO, K. MATSUGI and M. KOMATSU, *Mater. Sci. Eng.* **A350** (2003) 184.
149. Y. MAKINO, *New Ceramics* **10** (1997) 39.
150. H. TOMINO, H. WATANABE and Y. KONDO, *J. Jpn. Soc. Powd. Metall.* **44** (1997) 974.
151. O. A. GRAEVE, E. M. CARRILLO-HEIAN, A. FENG and Z. A. MUNIR, *J. Mater. Res.* **16** (2001) 93.
152. Y. C. WANG, Z. Y. FU and W. M. WANG, *Key Eng. Mater.* **249** (2003) 471.
153. Y. WANG and Z. FU, *Mater. Sci. Eng.* **B90** (2002) 34.
154. E. M. HEIAN, A. FENG and Z. A. MUNIR, *Acta Mater.* **50** (2002) 3331.
155. U. ANSELMI-TAMBURINI, S. GENNARI, J. E. GARAY and Z. A. MUNIR, *Mater. Sci. Eng.* **A394** (2005) 139.
156. U. ANSELMI-TAMBURINI, J. E. GARAY, Z. A. MUNIR, A. TACCA, F. MAGLIA, G. CHIODELLI and G. SPINOLO, *J. Mater. Res.* **19** (2004) 3263.